sharp cutoff are obtained. Higher beam width and lower ripple amplitude are achieved in the case of AP spaced perturbation systems. These antennas may find application as feeds

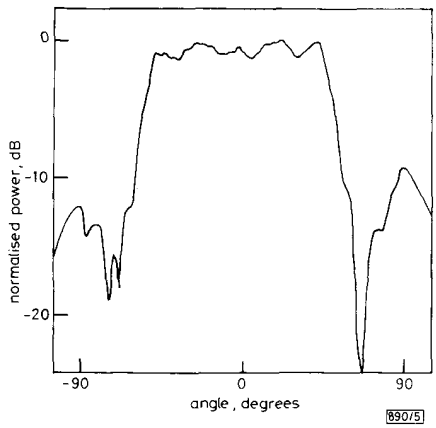

Fig. 5 *E-plane radiation pattern of the antenna with equal perturbation spacing*

$f = 9{\cdot}5$ GHz, $c = \lambda$, $d = 0{\cdot}6\lambda$

for deep cylindrical parabolic reflectors, where low spillover and uniform aperture illumination are required.

K. K. NARAYANAN
P. MOHANAN
K. VASUDEVAN
K. G. NAIR

Department of Electronics
Cochin University of Science & Technology
Cochin 682 022, India

2nd January 1991

References

1 KLOHN, K. L., HORN, R. E., JACOB, H., and FREIBERGS, E.: 'Silicon waveguide frequency scanning linear array antenna', *IEEE Trans.*, 1978, **MTT-26**, pp. 764–773
2 KOBAYASHI, S., LAMPE, R., MITTRA, R., and RAY, S.: 'Dielectric rod leaky-wave antennas for millimeter wave applications', *IEEE Trans.*, 1981, **AP-29**, pp. 822–824
3 NARAYANAN, K. K., VASUDEVAN, K., and NAIR, K. G.: 'A dielectric rod leaky-wave antenna with a conducting ground plane'. IEEE AP-S Int. Symp. Dig., 1988, pp. 366–369
4 NARAYANAN, K. K., MOHANAN, P., VASUDEVAN, K., and NAIR, K. G.: 'Prediction of radiation pattern of leaky-wave antennas'. IEEE AP-S Int. Symp. Dig., 1990, pp. 1847–1850

MATHEMATICAL APPROACH TO LARGE-SIGNAL MODELLING OF ELECTRON DEVICES

Indexing terms: Electron devices, Modelling

A general purpose mathematical approach is proposed for the large-signal modelling of microwave electron devices (e.g. MESFETs, bipolar transistors, diodes, etc.). The mathematical model, which is based on mild assumptions valid both for field effect and bipolar devices in typical large-signal operating conditions, can easily be identified through conventional measurements and is particularly suitable for nonlinear microwave circuit analysis based on harmonic balance techniques.

At present, the most popular design procedures for nonlinear microwave circuits (e.g. large-signal amplifiers, frequency converters, oscillators, etc.) are based on CAD techniques whose potentially high accuracy is strongly dependent on the availability of adequate large-signal models for electron devices (e.g. MESFETs, bipolar transistors, diodes, etc.). Usually, the modelling of the large-signal response of active devices is based on lumped nonlinear equivalent circuits. The identification of a nonlinear equivalent circuit, however, requires quite complex iterative procedures (with possible related convergence and accuracy problems) for the extraction of the model parameters from measured data.[1] Moreover, accuracy problems may arise at very high operating frequencies, owing to the approximations involved in the representation of intrinsically distributed phenomena through a 'lumped' equivalent circuit which is strongly dependent on the device structure.

As an alternative to equivalent circuits, suitable mathematical models can be used. The Volterra series, for instance, represents a possible alternative approach for the nonlinear dynamic modelling of electron devices; unfortunately it can be practically used only under weakly nonlinear operating conditions. Moreover, at microwave frequencies the direct measurement of Volterra kernels is practically almost impossible with the instrumentation now available.

In this Letter a new mathematical modelling approach is proposed which does not suffer from the limitations of the Volterra series; it is derived from the basic consideration that most types of electron devices, when described in a voltage-controlled form, exhibit only short-term 'memory' effects (i.e. the influence of 'past values' of the voltage on the instantaneous value of the current vanishes in a much shorter time than the inverse of the signal bandwidth). This property, which can be intuitively explained by considering that dynamic effects in electron devices are mainly associated to voltage-controlled charge-storage phenomena or very short transit times, is confirmed by experimental evidence. For instance, the current transient responses to voltage pulses applied either to the source or gate terminals of a GaAs MESFET whose typical operating frequencies are smaller than 20 GHz do not last longer than a few picoseconds (see Fig. 1). These values clearly

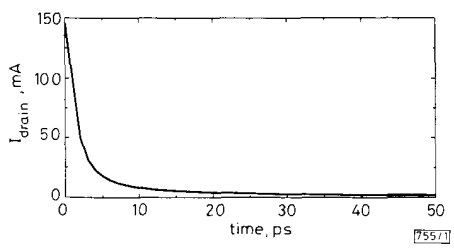

Fig. 1 *Drain current response of typical MESFET to a gate voltage pulse*

show that the duration of memory effects is much shorter than the inverse of the signal bandwidth in typical analogue applications. Similar results can be found for most types of electron devices (i.e. bipolar transistors, junction diodes, etc.) provided that a voltage-controlled description is used (otherwise the short-term memory assumption is not generally acceptable) and the intrinsic device (i.e. the 'active' part of the device) is not subject to dominant parasitic effects; this is generally true for devices used in monolithic circuits or discrete devices in 'bare-chip' form. With 'packaged' discrete devices, the package parasitics may 'slow down' the impulse response of the device and make the assumption of short-term memory not completely acceptable for very high operating frequencies; in such conditions good accuracy can still be achieved with the modelling approach proposed here provided that conventional techniques for 'de-embedding' from the linear package parasitics are used.[1]

Considering, for simplicity, a single-port device (but the same considerations are still valid for multiport devices provided that the following equations are interpreted in matrix terms) under large-signal dynamic operating conditions, the current i at any time instant t is nonlinearly dependent not only on the voltage $v(t)$ at the same instant, but also on past values $v(\tau)$ in the time interval $t - \tau_m \leq \tau < t$, where τ_m represents the practically finite duration of the 'memory' associated to dynamic phenomena in the device. The basic

assumption of a short-term memory implies that $\tau_m \ll (1/B)$, B being the practically finite bandwidth of the voltage applied at the device. In such conditions, according to the following considerations, the large-signal dynamic response of the device can be accurately approximated, at any time instant t, by a nonlinear current–voltage integral equation of the type:

$$i(t) = F_{DC}\{v(t)\} + \int_{t-\tau_m}^{t} g\{v(t), t-\tau\}[v(\tau) - v(t)]\, d\tau \qquad (1)$$

In eqn. 1 the nonlinear function F_{DC} clearly coincides with the static characteristic of the device because, in DC steady-state operation, the term $v(\tau) - v(t)$ in the integral is identically zero. So, the strictly dynamic phenomena are described by the convolution integral in terms of the quasistatic pulse-response function g, which is nonlinearly dependent on the instantaneous value assumed by the voltage v. The nonlinearly controlled convolution with respect to the dynamic signal variations $v(\tau) - v(t)$ is justified by the basic assumption of only short-term memory (i.e. $\tau_m \ll (1/B)$); in such conditions, in fact, the term $v(\tau) - v(t)$ is small enough to justify the superposition of dynamic effects defined by the integral in eqn. 1, even in the presence of large voltage amplitudes.

The current–voltage representation (eqn. 1) can be rigorously derived by applying the Volterra series under the hypothesis of only short-term memory for the device. The validity of eqn. 1 can be more intuitively justified if it is considered as the asymptotic limit of a discrete-time representation. In fact, because a finite bandwidth signal v is completely characterised over a finite time interval τ_m by a sufficiently large number N of samples, the current i at any time instant t can be expressed in the following form:

$$i(t) = F\{v(t), v_1(t), v_2(t), \ldots, v_N(t)\} \qquad (2)$$

where F is a nonlinear function of the voltages $v(t)$ and $v_k(t) = v(t - k\,\Delta\tau)$ with $k = 1, 2, \ldots, N$; the variables $v_k(t)$ are 'past' values of $v(t)$ which take into account the memory effects in the device through elementary delays $\Delta\tau = \tau_m/N$. Under the hypothesis of only short-term memory, the dynamic differences $v_k(t) - v(t)$ between the past values and the present one of the voltage are small, even in large-signal operation. Thus, in eqn. 2 the dependence of the present value $i(t)$ of the current on the past values $v_1, v_2, \ldots, v_N$ of the voltage can be linearised in the neighbourhood of the time-varying operating condition $v_1(t) = v_2(t) = \ldots = v_N(t) = v(t)$, as the past values are only slightly different from the present one $v(t)$. Accordingly, eqn. 2 can be expressed with good approximation in the form

$$i(t) = F_{DC}\{v(t)\} + \sum_{k=1}^{N} g_k\{v(t)\}[v(t - k\,\Delta\tau) - v(t)] \qquad (3)$$

where $g_k = (\partial F/\partial v_k)_{v_1 = \ldots = v_N = v(t)}$ and $F_{DC}\{v(t)\} = F\{v(t), \ldots, v(t)\}$. When considering the continuous-time domain (i.e. when $\Delta\tau \to 0$), eqn. 3 is clearly equivalent to eqn. 1.

When discrete-spectrum signals are considered, eqn. 1 can be more conveniently expressed, according to the well known properties of the Fourier transform, in the harmonic-balance oriented form

$$i(t) = F_{DC}\{v(t)\} + \sum_{k=-M}^{+M} \tilde{Y}\{v(t), \omega_k\} V_k e^{j\omega_k t} \qquad (4)$$

with

$$\tilde{Y}\{v(t), \omega\} = \int_0^{\tau_m} g\{v(t), \tau\}[e^{-j\omega\tau} - 1]\, d\tau \qquad (5)$$

where the V_ks represent the harmonic components of the voltage $v(t)$ at the angular frequencies ω_k (with $\omega_0 = 0$).

The term $\tilde{Y}$ in eqn. 4 represents a voltage and frequency-dependent 'dynamic' admittance which describes the purely dynamic phenomena (as $\tilde{Y}\{v(t), \omega\} = 0$ for $\omega = 0$) in the device in a quasistatic form, as it is nonlinearly dependent only on the instantaneous voltage $v(t)$; this is a quasistatic modelling approach which is justified by the hypothesis of short-term memory and is coherent with similar assumptions used in the derivation of some nonlinear equivalent circuits.[1,2] The mixed-mode (i.e. both time and frequency-domain) form of eqn. 4 can easily be used for circuit analysis by means of harmonic balance techniques. Otherwise, if a time-domain analysis is required, eqn. 1 can be directly used by applying conventional numerical integration techniques.[3]

The nonlinearly voltage-controlled dynamic admittance $\tilde{Y}\{v(t), \omega\}$ can be easily identified because it is related to the conventional bias-dependent small-signal admittance Y by a very simple relation. In fact, by considering a small sinusoidal voltage superimposed on a given DC bias voltage V_B, linearisation of eqn. 4 with respect to the small signals leads to the following expression:

$$\tilde{Y}[v, \omega_k] = Y[V_B, \omega_k] - g_{DC}[V_B] \qquad \text{with } V_B = v \qquad (6)$$

where $g_{DC} = (dF_{DC}/dv)_{V_B}$ is the DC differential conductance of the device.

Thus, once the DC characteristic F_{DC} and the small-signal admittance $Y[V_B, \omega_k]$ have been measured (or numerically evaluated by an accurate physical model)[4] for several different DC bias conditions and operating frequencies over the range of interest, by applying suitable interpolation techniques (e.g. spline or piecewise-linear interpolation) eqns. 4 and 6 can directly be used for the large-signal performance prediction in the framework of harmonic-balance circuit analysis.

The above-outlined modelling approach has been preliminarily tested in the large-signal performance prediction of GaAs MESFET amplifiers, by considering eqn. 4 as a matrix representation where i and v are two-dimensional vectors. In particular, validation tests have been carried out on an NEC NE71000 GaAs MESFET for which a set of experimental results under large-signal operating conditions and an extensively tested nonlinear equivalent circuit were already available.[5]

The results provided by the quasistatic mathematical model in the frequency range 2 to 20 GHz have been found to be at least as good as for the classical nonlinear equivalent circuit (see, for instance, the plots of the output power against input power in Fig. 2).

In comparison with equivalent circuits, our approach has the advantage of being a general purpose one as it is practically device independent; it is also easy to use because it does not require complex procedures for the parameter extraction from measured data. Moreover, our approach is suitable for

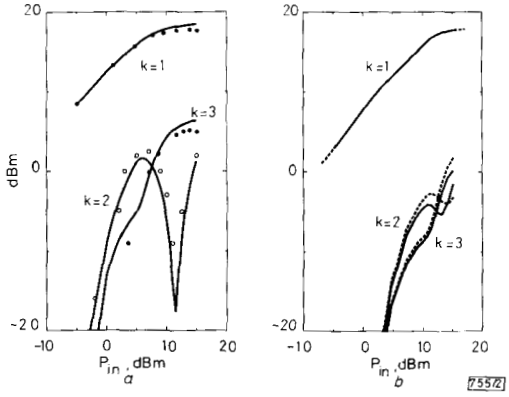

Fig. 2 *Plots of output powers associated to different order harmonics ($k = 1, 2, 3$) against input power P_{IN} for NEC NE71000 GaAs MESFET amplifier with sinusoidal input at two different frequencies*

Experimental results and those obtained by means of conventional equivalent circuit are in good agreement with performance by means of mathematical model proposed

○ ● Experimental results

– – – – Conventional equivalent circuit results

——— Performance predicted by proposed mathematical model

a $f = 26$ GHz

b $f = 10$ GHz

accurate modelling at high frequencies, as a lumped-element approximation of the frequency response of the device is not necessary.

F. FILICORI
G. VANNINI

Dipartimento di Elettronica, Informatica e Sistemistica
Università di Bologna, Viale Risorgimento 2—40136 Bologna, Italy

10th December 1990

References

1 HAIGH, D., and EVERARD, J. (Eds.): 'GaAs technology and its impact on circuits and systems' (Peter Peregrinus Ltd. on behalf of IEE, 1989)
2 RAUSCHER, C., and WILLING, H.: 'Simulation of nonlinear microwave FET performance using a quasi-static model', *IEEE Trans.*, 1979, **MTT-27**, pp. 834–840
3 FILICORI, F., and MONACO, V. A.: 'Computer-aided design of nonlinear microwave circuits', *Alta Frequenza*, 1988, **LVII**, (7), pp. 355–378
4 GHIONE, G., FILICORI, F., and NALDI, C.: 'Physical modeling of GaAs MESFET's in an integrated CAD environment: from device technology to microwave circuit performance', *IEEE Trans.*, 1989, **MTT-37**, pp. 457–468
5 SANGO, M., *et al.*: 'A GaAs MESFET large-signal circuit model for non-linear analysis'. IEEE MTT-S digest, 1988, pp. 1053–1056

ECG DATA COMPRESSION BY SUB-BAND CODING

Indexing terms: Data compression, Coding, Biomedical electronics

A data compression technique is presented for discrete-time electrocardiogram signals. The single lead electrocardiogram signal is decomposed into several multiresolution subsignals by using a quadrature mirror filter bank. The resultant subsignals are compressed according to their frequency contents using various coding methods, including a discrete cosine transform based technique and pulse code modulation with variable length coding. Compression ratios as high as 5·7 are obtained without introducing any visual distortion.

Introduction: Computerised electrocardiogram (ECG) processing systems have been widely used in ECG analysis.[1,2] The discrete-time ECG compression has become a necessity for many reasons. These include reducing the memory space in ECG data bases, reducing the transmission period of real time ECGs over telephone networks and increasing the recording time of the ambulatory devices.

Current data compression techniques for ECG signals can be classified as predictive coding (e.g. DPCM) methods and transform coding methods (see Reference 3 for an extensive survey of these methods). We present a sub-band coding based compression scheme for ECG signals. The ECG signal is split into subsignals by using a quadrature mirror filter bank in a tree structured fashion.

Sub-band coding has been successfully applied to speech[4] and image coding.[5,6] In the coding of sub-band signals, advantage is taken of the nonuniform distribution of energy in the frequency domain to judiciously allocate the bits to represent the sub-band signals. In our method the subsignal with the lowest frequency content is encoded by using a discrete cosine transform (DCT) based compression scheme[7] and the other subsignals are quantised using deadzone quantisers. The resulting data is coded using runlength coding of zero valued samples and variable length coding of the nonzero samples.

Description of procedure: Quadrature mirror filter bank (QMFB) is one of the building blocks used in multirate signal processing. It finds applications in situations where a discrete-time signal is to be split into a number of consecutive bands in the frequency domain. This division into frequency components removes the redundancy in the input and has the advantage that the number of bits used to encode each frequency band can be different, so that the encoding accuracy is always maintained at the required frequency bands.

The whole structure that is used to compress ECG signals is shown in Fig. 1. The single lead ECG signal is decomposed into four subsignals by using a QMF bank in a tree structured fashion and resulting stages of the tree are decimated by a factor of two. In the absence of quantisation errors, a QMF bank based tree structure provides perfect reconstruction, i.e.

$$y(n) = x(n - K) \qquad K \text{ an integer} \quad (1)$$

where $y(n)$ is the output and $x(n)$ is the input of the QMFB. This is because of the fact[8] that the lowpass, $H_l(\omega)$, and the high pass filter, $H_h(\omega)$ satisfy the following condition:

$$|H_l(\omega)|^2 + |H_h(\omega)|^2 = 1 \quad (2)$$

During the preprocessing of DI lead ECG data sampled at 500 Hz, it is observed that the energy of the ECG signals is highly concentrated at frequencies less than 62·5 Hz. Hence, at least a four frequency band filter bank is necessary. Each subband is then encoded according to criteria that are specific to that band. ECG waveforms depict that all the three bands except the lowest frequency band have noise-like variations, therefore they are coded using uniform quantisers. After quantisation, a code assignment procedure is realised using amplitude and runlength lookup tables which are derived by variable length coding from the histograms of quantised subband signals.

Transform coding was used in Reference 9 to compress discrete-time ECG signals. In our method we use a discrete cosine transform (DCT) based transform coding method to compress the sub-band signals with lowest frequency content. It is observed that the ECG signal energy is mainly concentrated in the lowest frequency band. Because of this, the

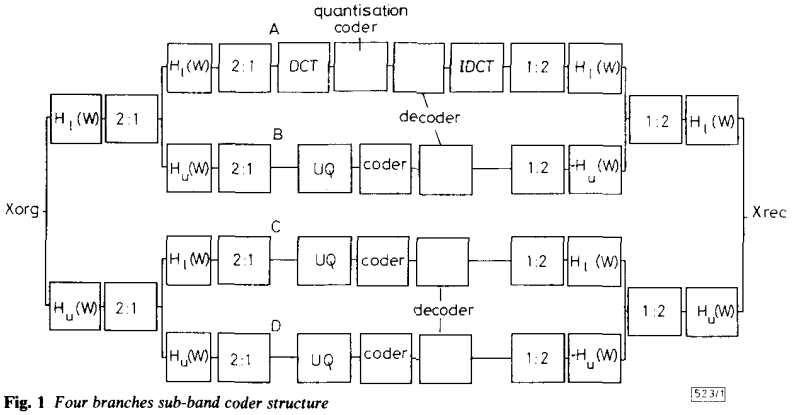

Fig. 1 *Four branches sub-band coder structure*